

# Irradiance Differences in the Violet (405 nm) and Blue (460 nm) Spectral Ranges among Dental Light-Curing Units

RICHARD B.T. PRICE, BDS, DDS, MS, PhD, FDS RCS (EDIN), FRCD (c)\*

DANIEL LABRIE, PhD<sup>†</sup>

FREDERICK A. RUEGGEBERG, DDS, MS<sup>‡</sup>

CHRISTOPHER M. FELIX, BSc<sup>§</sup>

## ABSTRACT

**Problem:** Previous studies identified nonuniformity in the irradiance at the tip end of a variety of dental light-curing units (LCUs) and correlated those differences with potential clinical implications, but the spectral dependence of the irradiance uniformity has not yet been addressed.

**Purpose:** This study examined the irradiance uniformity across emitting tips of LCUs at two emission wavelengths, 405 and 460 nm. Two broadband emission light units (quartz-tungsten-halogen [QTH] and plasma arc [PAC]), and four commercial light-emitting diode (LED)-type LCUs were examined.

**Materials and Methods:** The spectral radiant power from six LCUs was measured using a laboratory grade spectroradiometer (Ocean Optics, Dunedin, FL, USA). The spatial and spectral characteristics of irradiance across the emitting tips of these light units were recorded through 10-nm wide bandpass filters (centered at 405 nm [violet] or 460 nm [blue]) using a laser beam analyzer (Ophir-Spiricon, Logan, UT, USA). Irradiance distributions were reported using two-dimensional contour and three-dimensional isometric color-coded images. Irradiance uniformity at the tip end was determined using the Top Hat Factor (THF) for each filtered wavelength.

**Results:** Irradiance distributions from the QTH and PAC units were uniformly distributed across the tip end of the light guide, and THF values, measured through the 405 and 460-nm filters, were not significantly different. However, the three polywave LED units delivered non-uniform irradiance distributions with THF values differing significantly between the 405 and 460-nm emission wavelengths for each unit. Areas of nonuniformity were attributed to the locations of the various types of LED chips within the LCUs.

**Conclusion:** All three polywave LED units delivered a nonuniform irradiance distribution across their emitting tip ends at the two important emission wavelengths of 405 nm and 460 nm, whereas the broadband light sources (QTH and PAC) showed no evidence of spectral inhomogeneity at these wavelengths.

\*Professor, Department of Dental Clinical Sciences, Dalhousie University, Halifax, Nova Scotia, Canada

<sup>†</sup>Associate professor, Department Physics and Atmospheric Science, Dalhousie University, Halifax, Nova Scotia, Canada

<sup>‡</sup>Professor and section director, Dental Materials, The Medical College of Georgia, School of Dentistry Augusta, GA, USA

<sup>§</sup>Research assistant, Department of Dental Clinical Sciences, Dalhousie University, Halifax, Nova Scotia, Canada

### CLINICAL SIGNIFICANCE

Since the rate and extent of polymerization of photo activated restorative materials is highly dependent on delivering radiant energy at specific wavelengths, the nonuniform spectral distribution across the emitting tips of polywave light-emitting diode curing lights may affect the resulting properties of some photocured resins and their potential for long-term clinical success.

(*J Esthet Restor Dent* 22:363–378, 2010)

### INTRODUCTION

This is the second of two articles that examine the exitant irradiance from dental light curing units (LCUs). The first article showed that these units do not deliver a uniform irradiance across the emitting tip and that interchanging the light guide on the same LCU body affects power output, irradiance, and irradiance distribution.<sup>1</sup> The present article examines both the spatial and the spectral distribution of the exitant irradiance from quartz-tungsten-halogen (QTH), plasma arc (PAC), and light-emitting diode (LED) dental LCUs. Although the output from an LCU is often described in dentistry in terms of intensity or power density, this article will use the radiometric terms of radiant power (measured in watts), the spectral radiant power as a function of wavelength (watts/nm), and irradiance (radiant power/unit area) measured in mW/cm<sup>2</sup>.

To adequately cure a photoactivated resin, the spectral output from the LCU must match the wavelength-dependent photosensitivity of the photoinitiator used in

the resin.<sup>2</sup> This topic was not an issue in the past, when quartz-tungsten-halogen LCUs (e.g., Optilux 501, Kerr Corp., Orange, CA, USA) were used, because these LCUs deliver a broad spectrum of wavelengths ranging from ~375 to ~510 nm. The same concept is true for the more powerful PAC units. Recently, LED-curing units have become popular. Most contemporary LED-curing units contain single emission band LED<sub>blue</sub> chips that produce a very narrow band of wavelengths, with a typical full width at half maximum (FWHM) of ~25 nm. These units (e.g., Bluephase 16i, Ivoclar-Vivadent, Amherst, NY, USA) usually have an emission band in the 450 to 470-nm wavelength range and virtually no emission below 420 nm.<sup>3–5</sup> The LED<sub>blue</sub> units will efficiently cure resins containing camphorquinone (CQ), which is the most commonly used photoinitiator in dental resins. Unfortunately, CQ has a bright yellow color,<sup>6–8</sup> which can create chromatic problems when used as the photoinitiator in translucent or very light shades of resin. Consequently, some dental resins and bonding systems use

alternative photoinitiators that are not as chromogenic as CQ.<sup>7,9,10</sup> These alternative photoinitiators (e.g., monoacylphosphine oxide [Lucirin TPO] and 1-Phenyl 1,2-Propanedione) are activated by shorter wavelengths (below 420 nm) of light.<sup>6–12</sup> This requirement for shorter wavelengths has proved to be a problem for single emission band LED<sub>blue</sub> units and has led to the introduction of third-generation, polywave LED<sub>blue/violet</sub> LCUs<sup>3–5,10,12–19</sup> (e.g., G-Light GC America [Aslip, IL, USA], the Bluephase G2 and Bluephase 20i [Ivoclar-Vivadent], and VALO Ultradent Products Inc. [S. Jordan, UT, USA]). These polywave LED<sub>blue/violet</sub> LCUs use a combination of LED chips with different emission wavelengths to produce a spectral output that covers both the 440 and 470-nm range and the shorter wavelengths below 420 nm.<sup>5,13,18</sup> Polywave LED<sub>blue/violet</sub> LCUs have been reported to polymerize some resins to a greater extent than single emission band LED<sub>blue</sub> curing units delivering a similar irradiance.<sup>18</sup>

Three important factors associated with the design of an LCU affect

the irradiance and spectral distribution across the output face of the light tip: (1) the type, the physical size, and location of the light source within the LCU; (2) the optical components (lenses and reflectors) used to focus the light onto the entrance face of the light guide, or tooth if there is no light guide; and (3) the design of the light guide itself. Some LCUs use an elliptical reflector to focus a large optical beam to fill the proximal end of a rigidly held fiber-optic light guide. The power distribution of the radiation from the light source is not uniform and, depending on the quality of the reflector optics, may not be imaged uniformly at the corresponding focal point of the light guide entrance exists. This configuration causes uneven irradiance distribution at the emitting tip end. The light sources for both QTH and the PAC units can be described as thermal radiators generating broad emission spectra that are uniformly distributed across each point within the sources. The radiator nature of the sources and the optical arrangement result in an irradiance distribution across the emitting tip end that is the same at the two important emission wavelengths. In contrast, single emission band LED<sub>blue</sub> units deliver a relatively narrow emission spectrum with an FWHM of only ~25 nm. Thus, manufacturers

must use a combination of LED chips with different emission bands to deliver a broader emission spectrum. However, the location within the LCU of the multiple LED chips required to produce this broader spectral range of light may affect the spectral dependence of the irradiance distribution across the emitting tip of the LCU, and thus may also influence resin cure.

Many previous studies of the effect of different curing LCUs on resin polymerization used a dental radiometer to measure irradiance,<sup>20–25</sup> but this method has severe limitations.<sup>26,27</sup> When conducting research on curing lights, the ISO 4049 standard<sup>28</sup> recommends using a laboratory grade thermopile calibrated to a national standard, for example, National Institute of Standards and Technology (NIST; Gaithersburg, MD, USA), together with various filters to measure the radiant power delivered over certain wavelength ranges. An alternative method uses a spectroradiometer attached to an integrating sphere<sup>10,29</sup> to record both the spectral radiant power as a function of wavelength (watts/nanometer) and the total radiant power (watts). However, both the thermopile and the spectroradiometer-integrating sphere combination provide no information on the spatial

uniformity of the irradiance across the emitting tip of the LCU.

Laser beam analyzers are used to illustrate how the radiant power is apportioned across a light beam and have been used to characterize the light output from dental LCUs.<sup>1,15,30</sup> Using selected two-dimensional (2D) and three-dimensional (3D) color images of the irradiance across an emitting tip, it has been shown that several LCUs delivered a nonuniform, but radially symmetrical light beam. However, the spectral dependence of the irradiance distribution across the light beam was not reported.<sup>1,15,30</sup> Although laser beam analyzers can map the distribution of irradiance at the tip end, they do not discriminate among the various wavelengths within the light beam. Placing narrow bandpass filters in front of the camera and measuring irradiance distributions through the filtered transmission bands can overcome this limitation.

The purpose of this investigation was to measure and compare the irradiance distributions and degrees of uniformity across the tip ends of representative QTH, PAC, and LED-based LCUs at two emission wavelengths (violet, 405 nm and blue, 460 nm), which are within the absorption bands of the photoinitiators Lucirin TPO and CQ, respectively. Characterization was provided both in

**TABLE 1. LIGHT-CURING UNIT INFORMATION TOGETHER WITH RADIANT POWER AND TOP HAT FACTOR (MEAN ± STANDARD DEVIATION) OF ALL UNITS INVESTIGATED (N = 5 REPETITIONS).**

Light-curing unit and manufacturer	Curing unit type	Light guide entrance/exit diameter	Radiant power (mW) short wavelength LED	Radiant power (mW) long wavelength LED	Total radiant power* (mW)	THF <sup>†</sup> (460 nm)	THF <sup>†</sup> (405 nm)
Optilux 501 (Kerr Corp., Orange, CA, USA)	QTH	Standard 11/11 mm Regular power mode			586 ± 13	0.64 ± 0.01 <sup>Aa</sup>	0.64 ± 0.01 <sup>a</sup>
Sapphire (Den-Mat Holdings, Santa Maria, CA, USA)	PAC	Reverse turbo 5.5/10 mm			1142 ± 9	0.57 ± 0.01 <sup>Bb</sup>	0.57 ± 0.01 <sup>b</sup>
Bluephase 16i (Ivoclar Vivadent Inc., Amherst, NY, USA)	LED <sub>blue</sub>	Turbo 13/8 mm		679 ± 5	679 ± 5	0.49 ± 0.01	No light present
G-Light (GC America, Alsip, IL, USA)	Polywave LED <sub>blue/violet</sub>	Turbo 11/8 mm	23 ± 1	399 ± 1	423 ± 2	0.60 ± 0.01	0.44 ± 0.01
Bluephase G2 (Ivoclar Vivadent Inc.)	Polywave LED <sub>blue/violet</sub>	Standard 9/9 mm High power mode	110 ± 8	655 ± 6	765 ± 3	0.57 ± 0.01 <sup>B</sup>	0.37 ± 0.01
VALO Ultradent Products Inc. (S. Jordan, UT, USA)	Polywave LED <sub>blue/violet</sub>	Lens 10 mm High power mode	144 ± 3	807 ± 3 <sup>‡</sup>	950 ± 1	0.63 ± 0.01 <sup>A</sup>	0.49 ± 0.01

LED = light-emitting diode; PAC = plasma arc; QTH = quartz-tungsten-halogen; THF = Top Hat Factor.  
 \*The power values were all significantly different.  
<sup>†</sup>The THF values that were not significantly different (Fisher's PLSD  $p < 0.01$ ) within a column are indicated by similar superscript uppercase letter, and similar superscript lowercase letter indicates those within a row.  
<sup>‡</sup>This power value consists of the sum of the powers emitted by the 439 nm (180 mW) and 460 nm (627 mW) peak emission wavelength-LED chips in the VALO unit.  
 The short- and long-wavelength LED legends refer to the power from LED emission band centered at ~405 and ~460 nm.

terms of Top Hat Factor (THF) as well as distribution mapping of irradiance across the output tip of each LCU at the two wavelengths using 2D and 3D isometric color-coded images. The research hypotheses tested were that: (1) the degree of irradiance uniformity (as determined by the THF) at the 405 and 460-nm emission wavelengths is not significantly different for the QTH and PAC LCUs; (2) the location of the LED chips within the LCU and their emission wavelengths primarily define the tip end irradiance uniformity; (3) the degree of irradiance uniformity (as

determined by the THF) differs significantly between the 405 and 460-nm emission wavelengths for the polywave LED<sub>blue/violet</sub> LCUs; and (4) the spectral output, as measured using a spectroradiometer and an integrating sphere, does not describe the wavelength-dependent irradiance distribution across the tip end of the LCU.

#### MATERIALS AND METHODS

Table 1 lists the six LCUs investigated. These units were chosen to represent a wide variety of commercially available, contemporary dental LCUs: a QTH unit, a PAC unit, and four LED-type units.

The QTH and PAC units are broad-spectrum light sources; the Bluephase 16i is an example of a high power LED<sub>blue</sub>-type curing unit with a single, relatively narrow emission band. The G-Light, Bluephase G2, and VALO units are examples of polywave, third-generation LED<sub>blue/violet</sub>-type LCUs that have several emission bands. All except the VALO unit use a light guide, which positions the emitting chips at the distal end of the unit, and emits light through a lens. Where indicated, the batteries in the LCUs were fully charged before use.

### Spectral Radiant Power Measurement

The spectral radiant power was recorded five times in random order of LCUs using a laboratory grade spectroradiometer (USB 4000, Ocean Optics, Dunedin, FL, USA) and a 6-in integrating sphere (Labsphere, North Sutton, NH, USA) that had been calibrated to NIST standards. The absolute error of the spectroradiometer calibration was  $\pm 5\%$  (Ocean Optics). The tip end of the LCU was clamped over the entrance port of the integrating sphere to capture all of the light from the unit. Software (Spectra-Suite v2.0.146, Ocean Optics) running on a personal computer recorded the spectral radiant power from each unit from 350 to 550 nm. In addition, because of the absence of narrow emission bands for the QTH and PAC units, the radiant power in the 380 to 420-nm and 420 to 550-nm spectral range was calculated to estimate the total radiant power activating the Lucirin TPO and CQ photoinitiators, respectively. In the case of the polywave LED<sub>blue/violet</sub> units, where there were two or three different LED arrays with different, overlapping emission bands, the spectra were deconvoluted using software (Origin v7.0, OriginLab Corp., Northampton, MA, USA) on a personal computer to calculate the radiant power emitted from the

short, mid, and long emission wavelength LED chips. Deconvolution of the spectra was not required for the LED<sub>blue</sub> unit (Bluephase 16i), as this unit had only a single emission band that was used to calculate the radiant power.

### Irradiance Distribution Across the Tip End of the LCUs

The first article<sup>1</sup> described how the camera of a laser beam analyzer (Ophir-Spiricon LBA-USB-L070 Beam Profiler, Logan, UT, USA) was attached to an x-y-z positioning device mounted on an optical bench. To ensure that the beam images from all the LCUs could be accurately measured using the same x-y scale, the camera was held at the same fixed distance from the diffusive surface of a translucent, ground glass target (DG2X2-1500, Thor Laboratories, Newton, NJ, USA). The light-emitting end of each LCU was placed in contact with the diffusive (ground) surface of the target, the unit was turned on, and the resulting image was monitored on the computer screen. Prior to beam imaging, the pixel dimensions were calibrated to enable precise linear measurement of the images. Data were displayed graphically in real-time using software (LBA-USB-SCOR versus 4.84, Ophir-Spiricon) on a personal computer. Prior to beam imaging, the system was corrected

for ambient light and pixel response (UltraCal, Ophir-Spiricon), the LCU was then activated, and the lens iris was adjusted to use the full dynamic range of the beam profiler without saturation.

To compare the spectral irradiance uniformity of the six LCUs, the output from each unit was examined through a 10-nm-wide bandpass filter centered at 460 nm (ThorLabs FB460-10) or 405 nm (ThorLabs FB405-10). The central wavelengths for the two filters were selected so that they were within the FWHM of the absorption band for the Lucirin TPO (405 nm) and CQ (460 nm) photoinitiators, where significant absorption of radiant power occurs. Beam analysis was performed when the 405 or 460-nm bandpass filter was placed in front of the camera. In the case of the polywave LED units, the 460-nm filter allowed only light from the longer emission wavelength LED chips to reach the camera and the 405-nm filter allowed only light from the shorter emission wavelength LED chips to be imaged. Pilot studies of beam irradiance images recorded using narrow bandpass filters with central wavelengths on either side of those selected, indicated identical relative irradiance distributions to those obtained through the filters used in this study. These studies showed

that only the light from either the short or long emission wavelength LED chips reached the camera. The corresponding radiant power values for the short- and long-emission wavelength LED bands were then used to create an absolute scaled irradiance image of the light output obtained through the two filters. For the broadband spectra of the QTH and PAC units, the total radiant power emitted between 350 and 420 nm was used to scale the irradiance beam profile collected with the 405-nm filter, and total radiant power emitted between 420 and 550 nm was applied to the beam profile measured using the 460-nm filter. The software also calculated the THF across the active beam tip area for each LCU when imaged through the 405 or 460-nm filters. The radiant power values, beam images, and THF values were recorded five times for each unit, and the LCUs were tested in a random order through each filter.

To correlate the irradiance distribution measured at the LCU tip end with the LED chip arrangement within the LCU head, the light guide or lens was removed from the unit. The heads of the LED<sub>blue/violet</sub> units were then photographed, while powered, through an orange filter (Cure-Shield, Premier Dental, Plymouth Meeting, PA, USA). These pictures

were compared with their respective tip end beam profiles made with the light guide or lens in place and positioned similarly.

#### Analysis

Five beam profiles were obtained for each LCU through the 405 and 460-nm bandpass filters. Statistical analysis for the total radiant power values utilized a one-way analysis of variance (ANOVA), and a two-way ANOVA to examine the effect of the wavelength and LCU on the THF values. The Fisher's PLSD post hoc comparison test was used to examine pairwise differences in emitted power or THF values among the LCUs and between the 405 and 460 nm. All statistical testing was performed at a preset alpha of 0.01.

#### RESULTS

Figure 1 shows the spectral radiant power as a function of wavelength from the six LCUs together with the FWHM ranges of the Lucirin TPO and CQ absorption bands. The QTH and PAC units delivered a broad spectrum from ~375 to 510 nm, reaching a maximum value of 7.2 mW/nm at 477 nm for the QTH unit, and 14.4 mW/nm at 470 nm for the PAC unit. The single emission band of the LED<sub>blue</sub> type (Bluephase 16i) delivered a maximum value of 23.8 mW/nm at 456 nm, with no emission below 410 nm. Two of the

polywave LED<sub>blue/violet</sub> units (G-Light and Bluephase G2) displayed two emission bands that can be attributed to the short- and long-emission wavelength LEDs. The G-Light delivered a maximum spectral radiant power of 14.7 mW/nm at 468 nm and the Bluephase G2 delivered a maximum of 22.0 mW/nm at 463 nm. Figure 1 shows that one polywave LED<sub>blue/violet</sub> unit (VALO) displayed three emission bands centered at 405, 439, and 460 nm, which are attributed to the short, mid, and long-emission wavelength LED chips within this unit, respectively. On the high-output setting, the VALO delivered a maximum spectral radiant power of 21.5 mW/nm at 460 nm.

Table 1 presents the total radiant power emitted by each unit together with those from the short (~405 nm) and long (~460 nm) emission wavelength LED chips within each polywave LED<sub>blue/violet</sub> type unit. The THF values calculated from the irradiance distributions recorded through the short (405 nm) and long (460 nm) wavelength bandpass filters are also shown. The total radiant power from the LCUs ranged from an overall high of  $1,142 \pm 9$  mW for the PAC light, to  $423 \pm 2$  mW for the G-Light polywave LED<sub>blue/violet</sub> unit. One-way ANOVA indicated significant differences in the total radiant

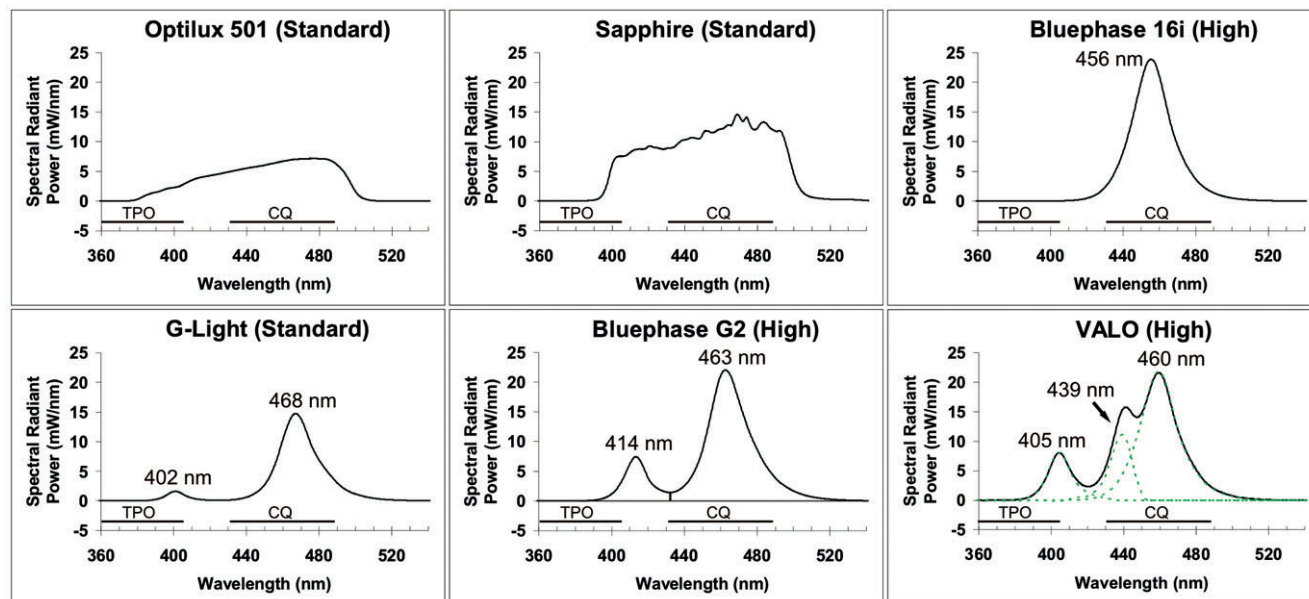


Figure 1. Spectral radiant power as a function of wavelength in the standard or high-output settings from the light-curing units (LCUs): Optilux 501, Sapphire, Bluephase 16i, G-Light, Bluephase G2, and VALO. The full width at half maximum of the absorption bands for the camphorquinone and Lucirin TPO photoinitiators are indicated by horizontal lines. Because of the very small overlap between the 414 and 463-nm light-emitting diode (LED) emission bands of the Bluephase G2 LCU, the solid vertical line at 432 nm gives the deconvolution of the two emission bands. The VALO spectrum (solid line) was deconvoluted into its three LED emission bands (green dashed lines).

power among the LCUs tested ( $p < 0.01$ ). Fisher's PLSD revealed that the radiant power values were significantly different among all the units. Because there was virtually no light output from the Bluephase 16i below 420 nm, this unit was omitted from the statistical comparisons. Two-way ANOVA showed that the THF values from the remaining five LCUs were significantly different and the three polywave LCUs were all significantly lower through the 405-nm filter compared with that of the 460-nm filter ( $p < 0.01$ ).

#### Irradiance Distribution from the QTH and PAC Units

Figure 2 shows representative 2D color-coded irradiance distributions across the emitting end of the QTH and PAC units when recorded through the 460- or 405-nm bandpass filter. These two LCUs deliver a relatively uniform irradiance at each emission wavelength and are characterized by THF values of  $0.64 \pm 0.01$  and  $0.57 \pm 0.01$ , respectively. Table 1 shows the results of Fisher's PLSD post hoc comparison tests for the THF values ( $p < 0.01$ ). There was no

significant difference between THF values calculated at 460- and 405-nm emission wavelengths for these two units.

#### Irradiance Distribution from the LED-type Units Obtained Using the 460-nm Bandpass Filter

Figures 3 and 4 show representative 2D and 3D color-coded irradiance distributions across the emitting tip end of the LED<sub>blue</sub> unit (Bluephase 16i) and polywave LED<sub>blue/violet</sub> units (G-Light, Bluephase G2 and VALO) when observed through the 460-nm bandpass filter. The Bluephase 16i

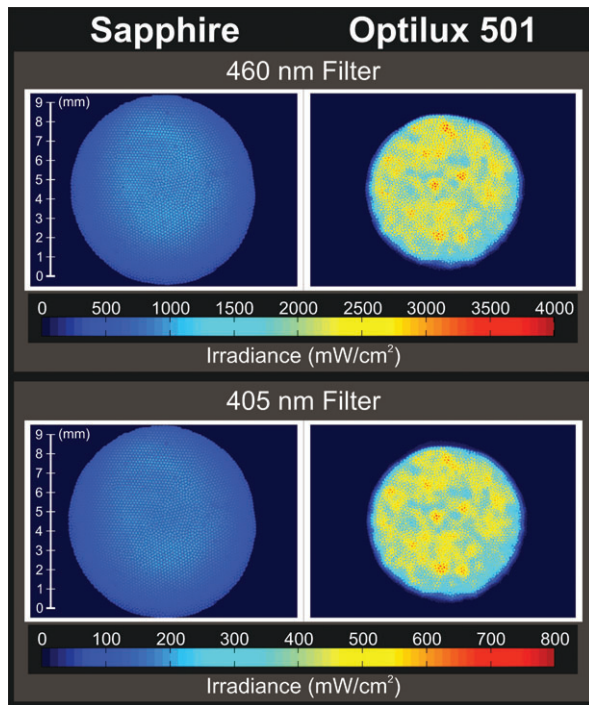


Figure 2. Two-dimensional isometric color-coded images of the irradiance distribution from the Optilux (quartz-tungsten-halogen) and Sapphire (plasma arc) units obtained using the 460- and 405-nm bandpass filters. Except for the irradiance scale, the irradiance distributions obtained using the two filters are nearly identical.

displayed a conical-like distribution of irradiance (THF:  $0.49 \pm 0.01$ ) and a high localized irradiance ( $\sim 3,700$  mW/cm<sup>2</sup>) over a small area at the center of the light guide. Table 1 shows that this unit delivered the lowest THF (0.49) at 460 nm among all units tested ( $p < 0.01$ ). Figures 3 and 4 also illustrate the nonuniform irradiance distribution for the longer emission wavelength across the tip end of the G-Light, Bluephase G2, and VALO LCUs. Fisher's PLSD showed that the VALO and the

Optilux 501 had the highest THF ( $0.64 \pm 0.01$  and  $0.63 \pm 0.01$ , respectively), and thus the most uniform beam irradiance at this emission wavelength.

#### Irradiance Distribution from the LED-type Units Obtained Using the 405-nm Bandpass Filter

Figures 5 and 6 show the irradiance distribution at the tip end of the LED<sub>blue</sub> unit (Bluephase 16i) and polywave LED<sub>blue/violet</sub> units (G-Light, Bluephase G2, and VALO) when observed through the

405-nm bandpass filter. As expected from Figure 1, the Bluephase 16i delivered no radiant power through this filter and no THF value was recorded in Table 1. Fisher's PLSD post hoc comparison tests showed that there were significant differences in THF values obtained using the 405 and the 460-nm bandpass filters for each polywave LED<sub>blue/violet</sub> unit and among units ( $p < 0.01$ ). The G-Light, Bluephase G2, and VALO polywave LED<sub>blue/violet</sub> units all delivered a measurable radiant power through the 405-nm filter, but the radiant power was not evenly distributed across the tip end of the units. When viewed through the 405-nm filter, the irradiance distribution for the G-light peaked at  $\sim 700$  mW/cm<sup>2</sup>, but was highly localized, occupying  $\sim 10\%$  of the optical beam cross section. The polywave LED<sub>blue/violet</sub> unit (Bluephase G2) delivered the greatest total irradiance (approximately 750 mW/cm<sup>2</sup>), but this value was delivered along only a small, peripheral segment of the light guide. The irradiance for the VALO was distributed more evenly across the beam and had the highest THF ( $0.49 \pm 0.01$ ) of the LED-type units at this emission wavelength. But because the power was distributed across a larger area of the tip, the maximum irradiance when viewed through the 405-nm filter was  $\sim 290$  mW/cm<sup>2</sup>.

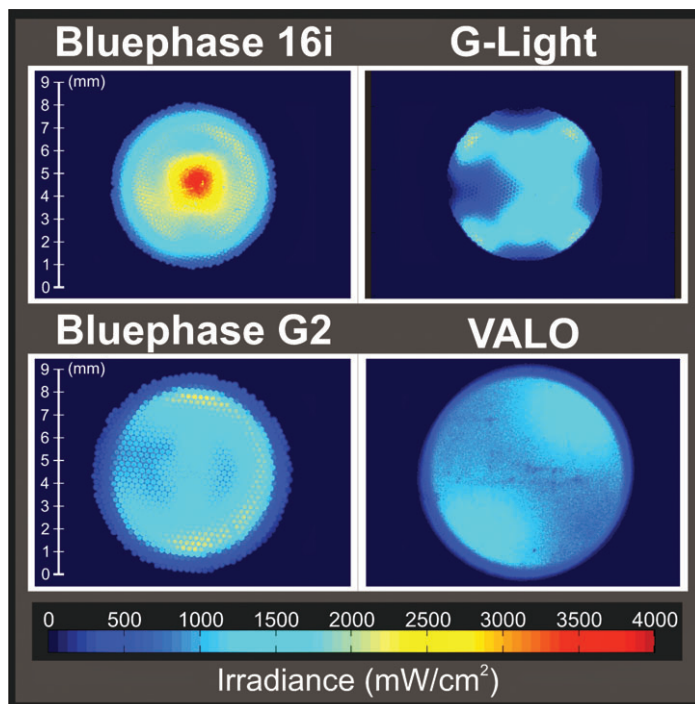


Figure 3. Two-dimensional isometric color-coded images of the irradiance distribution for Bluephase 16i, G-Light, Bluephase G2, and VALO units obtained using the 460-nm bandpass filter. Note the difference in irradiance distribution among the units.

#### Relationship Between LED Arrangement Within the LCU Head and Irradiance Distribution

Figure 7 shows photographs (top panel) of the polywave LED<sub>blue/violet</sub> units (G-Light, Bluephase G2, and VALO), obtained through an orange filter without the light guide or lens when the unit was activated. Each light's respective tip end irradiance distribution is also presented with the light guide or lens in place when viewed through the 405-nm (middle panel) and 460-nm (bottom panel) bandpass filters. Note the high spatial correlation between the irradiance

distribution collected through the 405 and 460-nm bandpass filters and the locations of the short-emission wavelength (A) and long-emission wavelength (C) LED chips within the LCU head.

#### DISCUSSION

The first hypothesis, that the degree of irradiance uniformity (as determined by the THF) at the 405- and 460-nm emission wavelengths are not significantly different for the QTH and PAC LCUs, was confirmed. Figure 2 shows that the QTH (Optilux 501) and PAC (Sapphire, Den-Mat Holdings,

Santa Maria, CA, USA) LCUs have uniform irradiance distributions across their tip ends at the two emission wavelengths. Furthermore, Table 1 shows that, for these units, the THF values were the same using both filters ( $p < 0.01$ ). This equivalence occurs because the light sources within the QTH and PAC units can be described as thermal radiators where the spectral radiant power is emitted over a very broad spectral range and it is the same at each location within the physical size of the light sources. The LCU's spectral radiant power is then filtered to deliver light in the 375- to 510-nm spectral range. As a result, it is not surprising to observe, in Figure 2, that the irradiance distributions measured using the two bandpass filters are virtually identical for the QTH and PAC units, and there was no significant difference in the THFs measured through the two bandpass filters.

The data also indicated that the second hypothesis, that irradiance uniformity from polywave LCUs depends on the position of the LED chips and their emission wavelengths, was also supported. Figures 3 to 7 show that the irradiance distribution measured at the emission wavelengths of 405 and 460 nm was nonuniform across the emitting end of all the polywave LED<sub>blue/violet</sub> units (G-Light, Bluephase G2, and VALO).

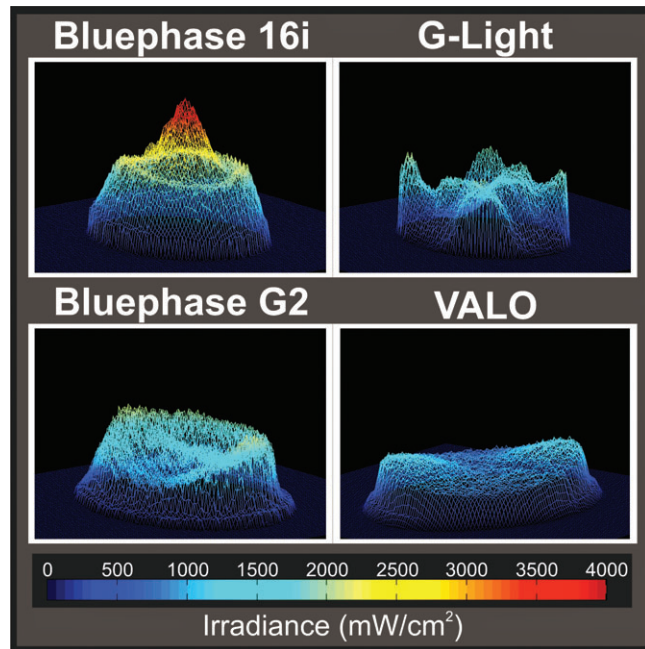


Figure 4. Three-dimensional isometric color-coded images of the irradiance distribution for Bluephase 16i, G-Light, Bluephase G2, and VALO units obtained using the 460-nm bandpass filter. Note the difference in irradiance distribution among the units.

Figure 7 shows that this nonuniformity was strongly correlated to the location of the specific short- (A) and long-emission wavelength (C) LED chips within the head of these polywave<sub>blue/violet</sub> LCUs. In each case, the short emission wavelength comes from only one (A) of the LED chips. This arrangement explains why the irradiance distribution in the shorter emission wavelength range was highly non-uniform for the polywave LCUs.

#### THF at 405 and 460 nm

The third research hypothesis, that the degree of irradiance uniformity (as determined by THF) differs

significantly among the LED units in the 405- and 460-nm spectral regions, was accepted. Two-way ANOVA by LCU and filter indicated significant differences in THF values among the LCUs and between those determined using the 405- and 460-nm bandpass filters ( $p < 0.01$ ). Although no significant difference between the THF values of the QTH (Optilux 501) or the PAC unit (Sapphire) obtained using the 405- or the 460-nm filters was found, there were significant differences for all LED units ( $p < 0.01$ ). For the 460-nm emission wavelength, the highest THF value, indicating

the most uniform beam irradiance, was found with the VALO unit (THF:  $0.64 \pm 0.01$ ), which utilizes only a lens over the bare LED chips, and the QTH unit (Optilux 501) when used with a standard light guide (THF:  $0.64 \pm 0.01$ ). The high THF value of 0.64 found for the QTH unit is attributed to the use of the 11-mm standard light guide. The high THF of 0.63, found for the polywave LED<sub>blue/violet</sub> unit (VALO), is attributed to the use of a well-matched LED source, reflector, and focusing lens. The conical-like shape irradiance distribution (THF:  $0.49 \pm 0.01$ ) from the LED<sub>blue</sub> unit (Bluephase 16i) imaged through the 460-nm filter is credited to the focusing effect of the 13/8-mm turbo light guide when attached to the Bluephase 16i. Table 1 shows that the THF values were all significantly lower for the polywave LEDs in the shorter wavelength range.

#### Spectral Dependence of the Irradiance Distribution Across the Tip End of the LCU

The fourth hypothesis was also accepted, which presumed that the spectral output measured with a spectroradiometer and an integrating sphere would not describe the wavelength-dependent irradiance distribution across the tip end of the LCU. Table 1 and Figure 7 shows that the locations of the A, B, and C-type LED chips dictate the irradiance distribution at the

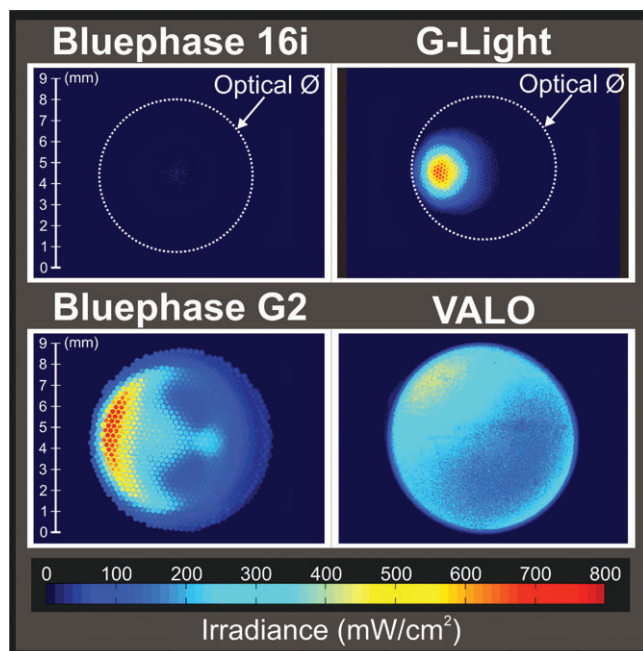


Figure 5. Two-dimensional isometric color-coded images of the irradiance distribution for Bluephase16i, G-Light, Bluephase G2, and VALO units obtained using the 405-nm bandpass filter. Note that no radiant power was measured for Bluephase 16i, as shown within the optical diameter  $\emptyset$ , and the strong asymmetry in the irradiance distribution for two of the three remaining units. The irradiance scale used here is five times smaller than those used in Figures 3 and 4.

emitting end of polywave LED<sub>blue/violet</sub> units; this is not the case for the QTH or PAC units. Although a spectroradiometer and integrating sphere are effective in determining the spectral radiant power, the spectroradiometer-integrating sphere combination measures the spectral output from the entire light source and is unable to detect any spatial variation within the light beam. Consequently, spectral radiant power values as a function of wavelength, such as those illustrated in Figure 1, are very misleading because the

reader may think that these wavelengths are delivered uniformly across the tip end of the LCU.

To be most effective when curing a resin, the spectral radiant power from the LCU must match the wavelength range that will activate the photoinitiators used in the resin.<sup>2,11</sup> Figure 1 shows the FWHM of the absorption bands for the Lucirin TPO and CQ, thus indicating which wavelengths will be most effective for curing. The 2D isometric images of the light outputs from the LCUs taken

through the 460-nm bandpass filter illustrate where light will most effectively activate CQ. Isometric images taken through the 405-nm bandpass filter illustrate where light will most effectively activate the alternative photoinitiators, for example, Lucirin TPO. Figure 1 depicts that the broad-spectrum QTH and PAC units and the poly-wave LED units deliver a broad spectrum of wavelengths that should activate resins containing either CQ or the alternative photoinitiator, Lucirin TPO. Figure 1 also shows that the single emission band LED-type unit, Bluephase 16i, does not emit the shorter wavelengths necessary to activate the alternative photoinitiator. The results from the beam profile analyses show that, although the three polywave LED<sub>blue/violet</sub> units tested delivered a broader emission spectra than the single emission band LED<sub>blue</sub>, the irradiance was not uniformly distributed across their emitting tip ends at the two important emission wavelengths of 405 and 460 nm. However, the broadband light units (QTH and PAC) showed no evidence of spectral inhomogeneity at these wavelengths.

#### Design Features of LCUs

Figures 3 to 7 demonstrate that a large variation in irradiance distribution exists at the two emission wavelengths. Unlike the QTH and PAC units, the irradiance

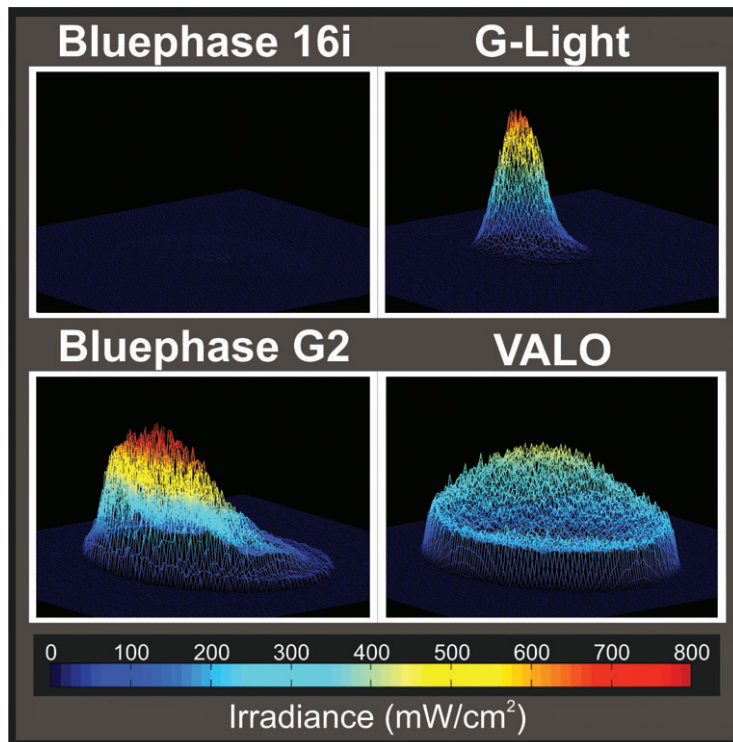


Figure 6. Three-dimensional isometric color-coded images of the irradiance distribution for Bluephase 16i, G-Light, Bluephase G2, and VALO units obtained using the 405-nm bandpass filter. Note that no radiant power was measured for Bluephase 16i and the strong asymmetry in the irradiance distribution for two of the three remaining units. The irradiance scale used here is five times smaller than those used in Figures 3 and 4.

distribution across the LCU emitting tip is highly nonuniform. In some regions across the emitting tip, the spectral emission of the polywave LED<sub>blue/violet</sub> units was the same as for the single emission peak LED<sub>blue</sub> unit. Although beam analyzers have been used previously to characterize the effects of the beam homogeneity from dental LCUs on resin polymerization,<sup>15,30</sup> the current report is the first to demonstrate the dramatic wavelength dependence of the irradiance

distribution across the tip end of current third-generation polywave LED<sub>blue/violet</sub> units. As both the rate and the extent of polymerization of photo-activated restorative materials are highly dependent on the resin receiving radiant energy at specific wavelengths, this large variation in irradiance distribution at the relevant wavelengths for photoinitiation will most likely affect the rate and extent of polymerization across the surface of a resin.

### Research, Clinical Implications, Study Limitations

The observation that beam profiles from some LCUs are not uniform at the wavelengths required for photoinitiation has important research and clinical implications. Handheld dental radiometers calculate irradiance based on a fixed aperture and assume that the LCU is delivering a uniform irradiance at the emitting tip within the spectral range required for photoinitiation. Because this assumption has been proven to be incorrect, data from the present study may help to explain why dental radiometers have been reported to be inaccurate by as much as 276%.<sup>26</sup> The spatial and spectral inhomogeneity in light output is a concern because some dental resins use photoinitiators that require shorter wavelengths of light.<sup>12,19</sup> When performing laboratory research using an LCU, the unit is typically clamped rigidly over the specimen. Although this fixturing reduces measurement variance, Figures 3 to 7 show that, when a polywave LED<sub>blue/violet</sub> LCU is used, not all of the resin will receive the same radiant energy at each LED emission wavelength. This discrepancy may affect measured depth of cure, microhardness, and degree of conversion values.

It is recognized that the current study did not evaluate all light units currently available. However, the specific unit types selected are

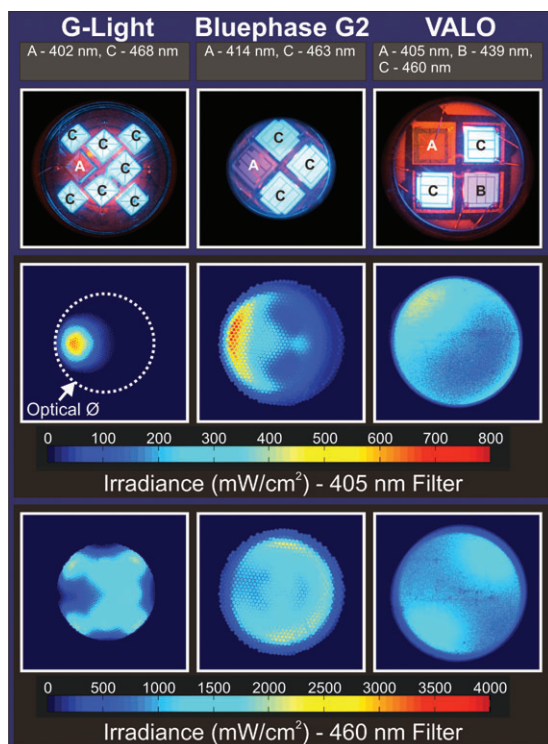


Figure 7. Top panel shows photographs of the polywave G-Light, Bluephase G2, and VALO LED<sub>blue/violet</sub>-type light-curing units (LCUs) taken through an orange filter showing the location of the different light-emitting diode (LED) chips: A = short emission wavelength chip delivering light to efficiently activate Lucirin TPO; B and C = LED chips delivering light in the long emission wavelength range that efficiently activate camphorquinone. Middle and bottom panels display two-dimensional isometric images of the irradiance distribution obtained using the 405- and 460-nm bandpass filters, respectively. Note the high spatial correlation between the isometric images and the A- and C-LED chip locations within the LCU heads.

thought to be representative of the wide variety available, and the results obtained are considered to be applicable to similar type LCUs. As the light unit is never fixed rigidly in one position in the mouth, conclusions of laboratory

studies comparing the performance of LCUs delivering nonuniform light beams at the photoinitiator absorption wavelengths, may not be clinically relevant. This shortcoming may be overcome in laboratory studies by a slight

movement of the curing light a few millimeters in the x-y coordinates. Such a simulation may average out the spatial and spectral variations in radiant power. For such conditions, the exposure time will have to be increased in order to deliver the same total energy to the entire resin surface.

#### CONCLUSIONS

Within the limitations imposed by the experimental design used in the current study, the following conclusions may be made:

1. The degree of irradiance uniformity (as determined by the THF) at the 405- and 460-nm emission wavelengths is not significantly different for the QTH and PAC units
2. The location of LED chips within the LCU and their emission wavelengths primarily define the spatial and spectral irradiance uniformity at the tip end
3. The degree of irradiance uniformity (as determined by the THF) differs significantly between the 405- and 460-nm emission wavelengths among the polywave LED<sub>blue/violet</sub> LCUs
4. The spectral output measured using a spectroradiometer and an integrating sphere does not describe the wavelength-dependent irradiance distribution across the tip end of the LCU

5. When characterizing light output from an LCU, the spectral radiant power as a function of wavelength, the irradiance distribution across the light beam at the relevant wavelengths for photoinitiation, and the THFs should be included.

#### DISCLOSURE AND ACKNOWLEDGEMENTS

The authors do not have any financial interest in the companies whose materials are included in this article.

Dalhousie University and a NSERC Discovery Grant # 298326 supported this study. Manufacturers of the LCUs used in this study are acknowledged for their kind donations. The authors wish to thank Mr John Fahey, statistician, Halifax, N.S., for his statistical support.

#### REFERENCES

- Price RBT, Rueggeberg FA, Labrie D, Felix CM. Irradiance uniformity and distribution from dental light curing units. *J Esthet Restor Dent* 2010;22:86–103.
- Nomoto R. Effect of light wavelength on polymerization of light-cured resins. *Dent Mater J* 1997;16:60–73.
- Bennett AW, Watts DC. Performance of two blue light-emitting-diode dental light curing units with distance and irradiation-time. *Dent Mater* 2004;20:72–9.
- Uhl A, Sigusch BW, Jandt KD. Second generation LEDs for the polymerization of oral biomaterials. *Dent Mater* 2004;20:80–7.
- Price RB, Felix CA, Andreou P. Evaluation of a dual peak third generation LED curing light. *Compend Contin Educ Dent* 2005;26:331–2, 4, 6–8. passim; quiz 48.
- Park YJ, Chae KH, Rawls HR. Development of a new photoinitiation system for dental light-cure composite resins. *Dent Mater* 1999;15:120–7.
- Neumann MG, Miranda WG, Jr, Schmitt CC, et al. Molar extinction coefficients and the photon absorption efficiency of dental photoinitiators and light curing units. *J Dent* 2005;33:525–32.
- Alvim HH, Alecio AC, Vasconcellos WA, et al. Analysis of camphorquinone in composite resins as a function of shade. *Dent Mater* 2007;23:1245–9.
- Ogunyinka A, Palin WM, Shortall AC, Marquis PM. Photoinitiation chemistry affects light transmission and degree of conversion of curing experimental dental resin composites. *Dent Mater* 2007;23:807–13.
- Ilie N, Hickel R. Can CQ be completely replaced by alternative initiators in dental adhesives? *Dent Mater J* 2008;27:221–8.
- Price RB, Felix CA. Effect of delivering light in specific narrow bandwidths from 394 to 515 nm on the micro-hardness of resin composites. *Dent Mater* 2009;25:899–908.
- Ye Q, Wang Y, Williams K, Spencer P. Characterization of photopolymerization of dentin adhesives as a function of light source and irradiance. *J Biomed Mater Res* 2007;80:440–6.
- Owens BM, Rodriguez KH. Radiometric and spectrophotometric analysis of third generation light-emitting diode (LED) light-curing units. *J Contemp Dent Pract* 2007;8:43–51.
- Uhl A, Mills RW, Jandt KD. Photoinitiator dependent composite depth of cure and Knoop hardness with halogen and LED light curing units. *Biomaterials* 2003;24:1787–95.
- Vandewalle KS, Roberts HW, Andrus JL, Dunn WJ. Effect of light dispersion of LED curing lights on resin composite polymerization. *J Esthet Restor Dent* 2005;17:244–54.
- Schattenberg A, Lichtenberg D, Stender E, et al. Minimal exposure time of different LED-curing devices. *Dent Mater* 2008;24:1043–9.
- Price RB, Ehrnford L, Andreou P, Felix CA. Comparison of quartz-tungsten-halogen, light-emitting diode, and plasma arc curing lights. *J Adhes Dent* 2003;5:193–207.
- Price RB, Felix CA, Andreou P. Third-generation versus a second-generation LED curing light: effect on Knoop micro-hardness. *Compend Contin Educ Dent* 2006;27:490–6. quiz 7, 518.
- Kim SY, Lee IB, Cho BH, et al. Curing effectiveness of a light emitting diode on dentin bonding agents. *J Biomed Mater Res* 2006;77:164–70.
- Lindberg A, Emami N, van Dijken JW. A Fourier transform Raman spectroscopy analysis of the degree of conversion of a universal hybrid resin composite cured with light-emitting diode curing units. *Swed Dent J* 2005;29:105–12.
- Soh MS, Yap AU. Influence of curing modes on crosslink density in polymer structures. *J Dent* 2004;32:321–6.
- Owens BM. Evaluation of curing performance of light-emitting polymerization units. *Gen Dent* 2006;54:17–20.
- Nalcaci A, Kucukesmen C, Uludag B. Effect of high-powered LED polymerization on the shear bond strength of a light-polymerized resin luting agent to ceramic and dentin. *J Prosthet Dent* 2005;94:140–5.
- Torno V, Soares P, Martin JM, et al. Effects of irradiance, wavelength, and thermal emission of different light curing units on the Knoop and Vickers hardness of a composite resin. *J Biomed Mater Res* 2008;85:166–71.
- Staudt CB, Krejci I, Mavropoulos A. Bracket bond strength dependence on light power density. *J Dent* 2006;34:498–502.
- Leonard DL, Charlton DG, Hilton TJ. Effect of curing-tip diameter on the accuracy of dental radiometers. *Oper Dent* 1999;24:31–7.
- Roberts HW, Vandewalle KS, Berzins DW, Charlton DG. Accuracy of LED and halogen radiometers using different light sources. *J Esthet Restor Dent* 2006;18:214–22; discussion 23–4.

28. International, Standard, 4049. Dentistry-polymer-based filling, restorative and luting materials. Geneva, Switzerland: International Organization for Standardization; 2000.
29. Bouschlicher M, Berning K, Qian F. Describing adequacy of cure with maximum hardness ratios and non-linear regression. *Oper Dent* 2008;33:312–20.
30. Vandewalle KS, Roberts HW, Rueggeberg FA. Power distribution across the face of different light guides and its effect on composite surface microhardness. *J Esthet Restor Dent* 2008;20:108–17; discussion 18.

---

*Reprint requests: Richard B.T. Price, BDS, DDS, MS, PhD, FDS RCS (EDIN), FRCD (c), Department of Dental Clinical Sciences, Dalhousie University, Halifax, Nova Scotia, B3H 1W2, Canada, Tel.: (902) 494-1226; Fax: (902) 494-1662; email: rbprice@dal.ca*

*MESH:  
Dentistry  
Curing Lights, Dental  
Image Processing, Computer-Assisted  
Imaging, Three-Dimensional  
Dental Equipment  
Lighting*

*This article is accompanied by commentary, "Irradiance Differences in the Violet (405 nm) and Blue (460 nm) Spectral Ranges among Dental Light-Curing Units," Kraig S. Vandewalle, DDS, MS, DOI 10.1111/j.1708-8240.2010.00369.x.*

Copyright of Journal of Esthetic & Restorative Dentistry is the property of Wiley-Blackwell and its content may not be copied or emailed to multiple sites or posted to a listserv without the copyright holder's express written permission. However, users may print, download, or email articles for individual use.